Available online at www.sciencedirect.com
SCIENCE DIRECT®
Journal of Computational Physics 208 (2005) 196–205
JOURNAL OF COMPUTATIONAL PHYSICS
www.elsevier.com/locate/jcp

A fast iterative solver for the variable coefficient diffusion equation on a disk

Ming-Chih Lai *, Yu-Hou Tseng

Department of Applied Mathematics, National Chiao Tung University, 1001, Ta Hsueh Road, Hsinchu 300, Taiwan

Received 7 September 2004; received in revised form 2 February 2005; accepted 9 February 2005
Available online 13 April 2005

Abstract

We present an efficient iterative method for solving the variable coefficient diffusion equation on a unit disk. The equation is written in polar coordinates and is discretized by the standard centered difference approximation under the grid arrangement by shifting half radial mesh away from the origin so that the coordinate singularity can be handled naturally without pole conditions. The resultant matrix is symmetric positive definite so the preconditioned conjugate gradient (PCG) method can be applied. Different preconditioners have been tested for comparison, in particular, a fast direct solver derived from the equation and the semi-coarsening multigrid are shown to be almost scalable with the problem size and outperform other preconditioners significantly. The present elliptic solver has been applied to study the vortex dynamics of the Ginzburg–Landau equation with a variable diffusion coefficient.

Keywords: Variable diffusion equation; Polar coordinates; Iterative method; Ginzburg–Landau vortices

1. Introduction

The variable coefficient elliptic equation arises in many physical applications. The heat transfer in heterogeneous material where the thermal conductivity depends on the position is one of the classical examples. Another example comes from the Ginzburg–Landau of superconductivity. When a superconductor contains impurities, it is quite natural to consider the inhomogeneous coherence length in the Ginzburg–Landau equation. Thus, a nonlinear variable elliptic-type equation must be solved where the variable coefficient represents the coherence length for superconducting electrons in a material [5]. Motivated by the

* Corresponding author. Fax: +88 6357 24679.
E-mail address: mclai@math.nctu.edu.tw (M.-C. Lai).

0021-9991/$ - see front matter © 2005 Elsevier Inc. All rights reserved.
doi:10.1016/j.jcp.2005.02.005

above problems, in this paper, we consider the following variable coefficient diffusion equation written in polar coordinates on a 2D unit disk $\Omega = \{(r,\theta)|0 < r < 1,\ 0 \leqslant \theta < 2\pi\}$ as

$$-\frac{1}{r}\left[\frac{\partial}{\partial r}\left(\beta r\frac{\partial u}{\partial r}\right)+\frac{\partial}{\partial \theta}\left(\frac{\beta}{r}\frac{\partial u}{\partial \theta}\right)\right] = f(r,\theta) \quad \text{in } \Omega, \tag{1}$$

$$u(1,\theta) = g(\theta) \quad \text{on } \partial\Omega, \tag{2}$$

where the diffusion coefficient $\beta(r,\theta) > 0$ is inhomogeneous in the disk.

When we solve Eq. (1) numerically, the first issue called the coordinate singularity arises. This is because the equation is not valid at $r = 0$ when it is written in polar coordinates. In [12], the first author discretized the Poisson equation (a special case of $\beta(r,\theta) = 1$ in Eq. (1)) by using the standard centered difference scheme under a polar grid by shifting a half radial mesh away from the origin. It was found that the method handles the coordinate singularity without special treatment and the resultant matrix equation is simpler than the traditional method described in [18]. Furthermore, the desired accuracy has been preserved. Mohseni and Colonius [14] have used similar grid arrangements to handle the coordinate singularities in finite difference and pseudo-spectral methods and have applied them to Bessel's equation and compressible Navier–Stokes equations.

Another standard technique to solve the Poisson equation on a disk is as follows. We first write the solution as a truncated Fourier series in the θ direction and obtain a set of Fourier mode equations. Then those ordinary differential equations of Fourier coefficients are solved by either finite difference or spectral methods. Once again, in order to have the desired regularity and accuracy, most of the numerical methods including the finite difference method [10], or spectral method [7,9,17] need to impose appropriate conditions on the solution at the coordinate singularity. The accuracy of the numerical methods depends greatly on the choice of pole conditions. Until recently, different numerical methods without pole conditions have been proposed as well [6,8,13].

The numerical solution of the variable coefficient diffusion equation (1) is another different story. Since now the elliptic equation has a variable diffusion coefficient, we are unable to write the solution as Fourier series expansion. Thus, the fast Fourier transform (FFT) cannot be called directly. Furthermore, Eq. (1) is not a separable type, the resultant linear system after the discretization cannot be solved directly by the fast direct solvers such as those provided in public software package – FISHPACK [3]. The goal of this paper is to develop an efficient iterative method for solving the variable coefficient diffusion equation (1).

The rest of this paper is as follows. In Section 2, we introduce the finite difference discretization to Eq. (1) and discuss two efficient preconditioners for the resultant linear system. The numerical results include the accuracy check and the detailed performance comparison for different preconditioners are also shown in Section 2. We then apply the present elliptic solver to study the vortex dynamics of the Ginzburg–Landau equation with a variable diffusion coefficient in Section 3. Some conclusion are given in Section 4.

2. Finite difference discretization

We use the same grid points in the radial direction as in [14,12] by defining

$$r_i = (i-1/2)\Delta r, \quad r_{i-1/2} = r_i - \Delta r/2, \quad r_{i+1/2} = r_i + \Delta r/2 \tag{3}$$

and in the azimuthal direction

$$\theta_j = j\Delta\theta, \quad \theta_{j-1/2} = \theta_j - \Delta\theta/2, \quad \theta_{j+1/2} = \theta_j + \Delta\theta/2, \tag{4}$$

where $\Delta r = 2/(2M+1)$ and $\Delta\theta = 2\pi/N$. By the choice of the radial mesh width, the boundary values are defined on the grid points. Let the discrete values be denoted by $u_{ij} \approx u(r_i,\theta_j)$, $f_{ij} \approx f(r_i,\theta_j)$, and $g_j = g(\theta_j)$. Using the centered difference method to discretize equation (1), we have

$$-\frac{1}{r_i}\left[\left(r_{i+1/2}\beta_{i+1/2,j}\frac{u_{i+1,j}-u_{i,j}}{\Delta r} - r_{i-1/2}\beta_{i-1/2,j}\frac{u_{i,j}-u_{i-1,j}}{\Delta r}\right)\Big/\Delta r + \left(\frac{\beta_{i,j+1/2}}{r_i}\frac{u_{i,j+1}-u_{i,j}}{\Delta\theta} - \frac{\beta_{i,j-1/2}}{r_i}\frac{u_{i,j}-u_{i,j-1}}{\Delta\theta}\right)\Big/\Delta\theta\right] = f_{i,j}. \tag{5}$$

Among the above representations, the numerical boundary values are given by $u_{M+1,j} = g_j$, and $u_{i0} = u_{i,N}$, $u_{i1} = u_{i,N+1}$ since u is 2π periodic in θ. At $i = 1$, we immediately observe from (3) that $r_{1/2} = 0$, so the coefficient of u_{0j} is zero. This implies that the scheme does not need any extrapolation for the inner numerical boundary value u_{0j} so that there is no pole condition needed. It is also easy to check that the matrix of linear equations (5) is symmetric and positive definite so the preconditioned conjugate gradient methods can be applied.

For the Neumann problem, we still use the same grid described in (3) but with different choice of $\Delta r = 1/M$. With the choice of this mesh width, the discrete values of u are defined midway between boundary so that the first derivative can be centered on the grid points.

2.1. Fast direct solver as a preconditioner

In this subsection, we derive a preconditioner which can be applied to the conjugate gradient method to solve the linear system (5). Our intention is to construct a preconditioner P such that the inversion of the matrix P can be done by available fast direct solvers such as FFT. One natural choice is to average the variable coefficient in Eq. (1) so that a separable PDE is formed. More precisely, the preconditioner can be constructed from the equation

$$-\frac{1}{r}\left[\frac{\partial}{\partial r}\left(\bar{\beta} r\frac{\partial u}{\partial r}\right) + \frac{\partial}{\partial\theta}\left(\frac{\bar{\beta}}{r}\frac{\partial u}{\partial\theta}\right)\right] = f(r,\theta), \tag{6}$$

where the coefficient

$$\beta(r) = \frac{1}{2\pi}\int_0^{2\pi}\beta(r,\theta)\,\mathrm{d}\theta. \tag{7}$$

Since the new diffusion coefficient β is a function of r, the above PDE is separable. Thus, the inversion of the preconditioner can be efficiently done by fast direct solvers such as FFT or block cyclic reduction algorithm [1].

2.2. Semi-coarsening multigrid as a preconditioner

Multigrid method is known to be an efficient solver for the linear system arising from discretized elliptic equations. Its main idea consists of applying simple relaxation on the fine grid (which damps the high-frequency errors quickly) and correcting the solution on the coarser grid (which the low-frequency errors can be represented accurately). Recently, Schaffer [16] developed an efficient semi-coarsening multigrid method for symmetric and nonsymmetric elliptic PDEs with highly discontinuous and anisotropic coefficients in two- and three-dimensional Cartesian domains. Based on Schaffer's work, Baldwin et al. [2] applied the semi-coarsening multigrid algorithm to the linear systems arising from radiation-hydrodynamics problems and made a detailed comparison with other iterative solvers. For the problems (the diffusion equation

with variable coefficients) considered there, the authors showed that the multigrid algorithms scale almost perfectly. In other words, the iteration count of V-cycle is almost independent of problem size. In their work, the multigrid algorithm is not only used alone as an efficient solver but also used as a preconditioner in the PCG method.

In this paper, we apply a similar multigrid V-cycle as in [2] to our resultant linear system (5) on the polar grid. The present method uses a combination of semi-coarsening in the θ direction with red/black line relaxation in the r direction. That is, we only do multigrid and coarsen the grid in the θ direction and keep the resolution in the r direction fixed. This is a quite natural choice since if we coarsen the radial grid instead, then the coarser grid would not coincide with the fine grid based on our radial grid arrangement (3). One should also note that the red/black line relaxation updates the solution by solving tridiagonal linear systems at all red lines (even index j lines) first and then follows a similar update for the black lines (odd index j lines). Since there is no dependence between lines of the same color, those tridiagonal solvers can be performed in parallel. The restriction (fine to coarse) and prolongation (coarse to fine) operators are the conventional full weighting and linear interpolation, respectively. In this work, we use the above multigrid as a preconditioner in the PCG method. That is, in the preconditioning step, we apply a single V(1,1)-cycle (one red/black line pre-relaxation and one black/red line post-relaxation) to solve the residual equation.

2.3. Numerical results

In this subsection, we perform several numerical tests for the presented method. Table 1 shows the maximum errors of the method for three different test examples as

1. $u = e^{r(\cos\theta+\sin\theta)}, \quad \beta = r^2\sin^2\theta + r\cos\theta + 1.1.$
2. $u = \sin(r\cos\theta)\sin(r\sin\theta), \quad \beta = e^{r(\cos\theta+\sin\theta)}.$
3. $u = r^5\cos^3\theta\sin^2\theta/3 + r^3\cos^2\theta\sin\theta + r\cos\theta + 1, \ \beta = 0.1(r^2\cos\theta\sin\theta + 1).$

The right-hand side functions are obtained by substituting the solutions into Eq. (1).

In all our tests, we use M grid points in the radial direction and $N = 2M$ points in the azimuthal direction. The rate of convergence is computed by the formula $\log_2\left(\frac{E_{M/2}}{E_M}\right)$, where E_M is the relative maximum error with radial resolution M. All the results are obtained by solving the linear system (5) using PCG with the fast direct solver (6) as the preconditioner. The initial guess of the iteration is set to be $u_{ij} = 1$ everywhere, and the tolerance of residual is 10^{-8}. One can see from Table 1 that indeed our scheme preserves clean second-order accuracy.

Table 1
The maximum errors of three different solutions u with different diffusion coefficients β for Eq. (1)

M	16	32	64	128
Ex. 1				
Error	1.160E − 03	2.828E − 04	6.961E − 05	1.726E − 05
Rate	–	2.04	2.02	2.01
Ex. 2				
Error	2.941E − 03	7.043E − 04	1.720E − 04	4.247E − 05
Rate	–	2.07	2.03	2.02
Ex. 3				
Error	1.089E − 03	2.742E − 04	6.818E − 05	1.697E − 05
Rate	–	1.99	2.01	2.01

Table 2
The performance comparison for using different preconditioners

M	BJ	SSOR	IC	FDS	SMG
16	70 (0.23)	39 (0.22)	28 (0.09)	28 (0.11)	5 (0.15)
32	133 (0.58)	60 (0.48)	53 (0.24)	33 (0.28)	5 (0.23)
64	240 (4.61)	93 (3.19)	103 (2.12)	36 (0.85)	5 (0.41)
128	478 (43.39)	147 (25.35)	195 (20.21)	36 (3.40)	5 (1.54)

The first number represents the number of iterations while the number in parentheses represents the CPU time in seconds.

Table 2 shows the number of iterations and the CPU time in seconds needed for solving the solution of Example 1 by PCG method with different preconditioners. Those preconditioners include block Jacobi (BJ), symmetric successive over relaxation (SSOR), incomplete Cholesky factorization (IC), the fast direct solver (FDS), and the semi-coarsening multigrid (SMG). One can see that the fast direct solver and the semi-coarsening multigrid are almost scalable with the mesh size and outperform other preconditioners significantly. The performance for other examples show the same conclusion so we omit here. The SMG preconditioner performs even better than FDS in terms of the iteration count and CPU time.

3. Simulation of Ginzburg–Landau equation with a variable diffusion coefficient

In this section, we apply the present iterative elliptic solver to study the stable solutions of the following Ginzburg–Landau equation (GLE) with a variable diffusion coefficient in a unit disk $\Omega = \{r^2 = x^2 + y^2 < 1\}$

$$\frac{\partial u}{\partial t} = \frac{1}{a(\mathbf{x})}\nabla \cdot (a(\mathbf{x})\nabla u) + \frac{1}{\varepsilon^2}(1 - |u|^2)u \quad \text{in } \Omega, \tag{8}$$

$$u(\mathbf{x}, 0) = u_0(\mathbf{x}) \quad \text{in } \Omega, \tag{9}$$

$$\frac{\partial u}{\partial r} = 0 \quad \text{on } \partial\Omega. \tag{10}$$

This 2D model approximates the three-dimensional Ginzburg–Landau equation with constant coherence length in a very thin variable superconducting film where the positive coefficient $a(\mathbf{x})$ characterizes the variable thickness [5]. The solution u is a complex-valued function representing the order parameter and the parameter ε is a small positive number. Note that, we use the Cartesian shorthand $\nabla \cdot (a(\mathbf{x})\nabla u)$ to represent the variable diffusion operator described as (1) in polar coordinates.

In this simulation, we want to study the steady equilibrium solutions of GLE (8). In particular, we will focus on seeking the stable solutions with vortices. The vortices are the topological defects which are zeros of the complex scalar field u with nonzero integer winding numbers. Readers who are interested in the theory of Ginzberg–Landau vortices can refer to the book [4].

Throughout this section, we use the backward difference in time to discretize the Ginzburg–Landau equation (8)

$$\frac{u^{n+1} - u^n}{\Delta t} = \frac{1}{a(\mathbf{x})}\nabla \cdot (a(\mathbf{x})\nabla u^{n+1}) + \frac{1}{\varepsilon^2}(1 - |u^n|^2)u^{n+1} \quad \text{in } \Omega, \tag{11}$$

$$\frac{\partial u^{n+1}}{\partial r} = 0 \quad \text{on } \partial\Omega. \tag{12}$$

Thus, at each time step, a variable diffusion coefficient elliptic equation with Neumann boundary on a disk arises and can be solved by the efficient iterative solver described in the previous section. In the following tests, we choose the initial condition as

$$u_0(r,\theta) = \tanh\left(\frac{r}{\varepsilon}\right) e^{im\theta}, \tag{13}$$

which is an approximate vortex solution with winding number m. As mentioned before, we like to investigate the dynamics of this vortex solution and its final equilibrium.

In all runs, we use 64×128 grid points in the radial and azimuthal directions, and the time step $\Delta t = 1/320$. The parameter $\varepsilon = 0.1$ and the winding number of initial vortex is $m = 3$. Fig. 1 shows the contour plots of the magnitude $|u|$ for the constant diffusion case $a(\mathbf{x}) = 1$ at different times. One can observe that the initial vortex with winding number $m = 3$ at the center splits into three vortices with winding number one and then migrate to the boundary gradually. At a later time, the three vortices are completely absorbed by the boundary and the solution becomes a constant state $|u| = 1$ eventually. This vortex dynamics is not new and has been confirmed, for instance, theoretically [11] and numerically [15]. One should also note that this final equilibrium state is nothing but the global minimizer of the Ginzburg–Landau free energy

$$E(u) = \int_\Omega \left\{\frac{1}{2}|\nabla u|^2 + \frac{1}{4\varepsilon^2}(1-|u|^2)^2\right\} a(\mathbf{x})\,d\mathbf{x}, \tag{14}$$

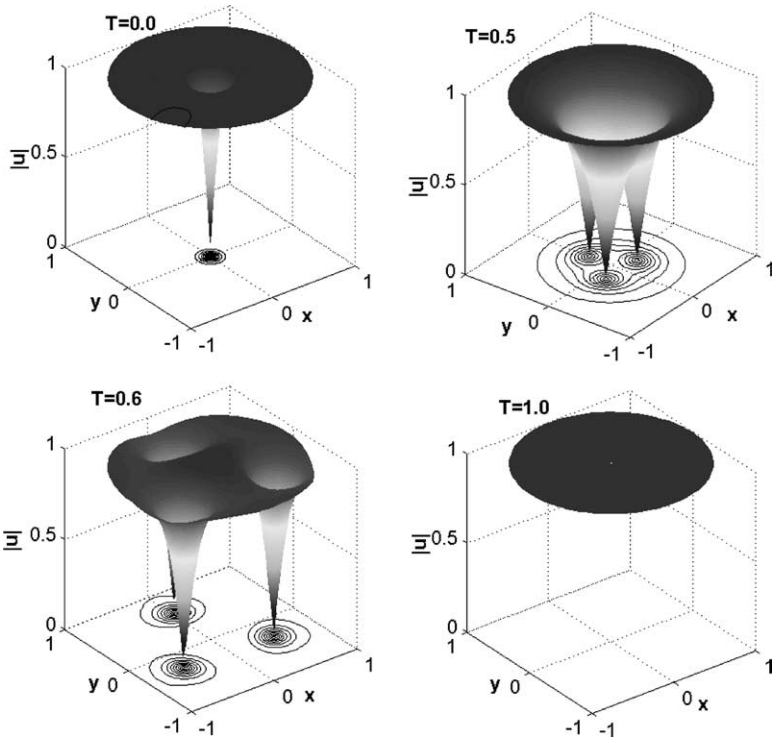

Fig. 1. The contour plots of $|u|$ at different times for the constant diffusion $a(\mathbf{x}) = 1$ case.

where the term $|\nabla u|^2$ in polar coordinates has the form

$$|\nabla u|^2 = \left|\frac{\partial u}{\partial r}\right|^2 + \frac{1}{r^2}\left|\frac{\partial u}{\partial \theta}\right|^2. \tag{15}$$

Fig. 2 shows that the Ginzburg–Landau energy is decreasing in time and becomes zero finally.

For the variable diffusion coefficient case, the vortex dynamics and stability are completely different from the constant diffusion case. Fig. 3 shows the different time contour plots of the magnitude $|u|$ for the case of variable diffusion $a(r,\theta) = (r^2\cos\theta\sin\theta + 1)\,e^r$. The initial condition is still as in (13) with winding number $m = 3$. Unlike the constant diffusion case, the central vortex now splits into five vortices in which one vortex stays at the center and four of them migrate to the boundary. Later, those surrounding four vortices are completely absorbed by the boundary while the vortex at the center remains. Fig. 4 shows that the free energy is decreasing in time and becomes a nonzero constant eventually. Therefore, by choosing the variable coefficient appropriately, we are able to stabilize the Ginzburg–Landau vortex which is exactly the same phenomena predicted by the theory [5]. In physics, this is called the pinning effect when a vortex is trapped by some defect of the conductor.

It is very interesting to mention that during the transition the winding number of the central vortex becomes $m = -1$ while the winding number of the surrounding four vortices are all $m = 1$. To see this, we plot the vector fields of real and imaginary parts for $u/|u|$ at $T = 0.5$ in Fig. 5(a). The final plots for the real and imaginary parts of $u/|u|$ near the vortex center (along the circle $r = 5\Delta r/2$) are shown in Fig. 5(b). The graphs of real and imaginary parts are exactly the functions $-\cos\theta$ and $\sin\theta$, respectively. Since we have

$$\frac{u}{|u|} = -\cos\theta + i\sin\theta = e^{i[(-1)\theta+\pi]} \tag{16}$$

one can immediately conclude that the winding number of the stable vortex is indeed $m = -1$.

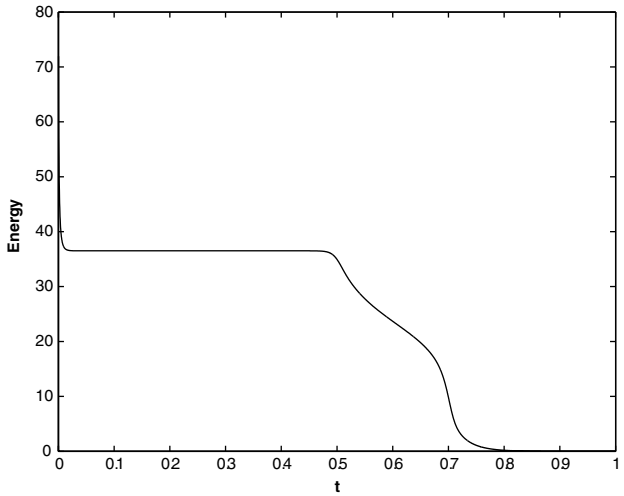

Fig. 2. The time evolution of Ginzburg–Landau energy for the constant diffusion case.

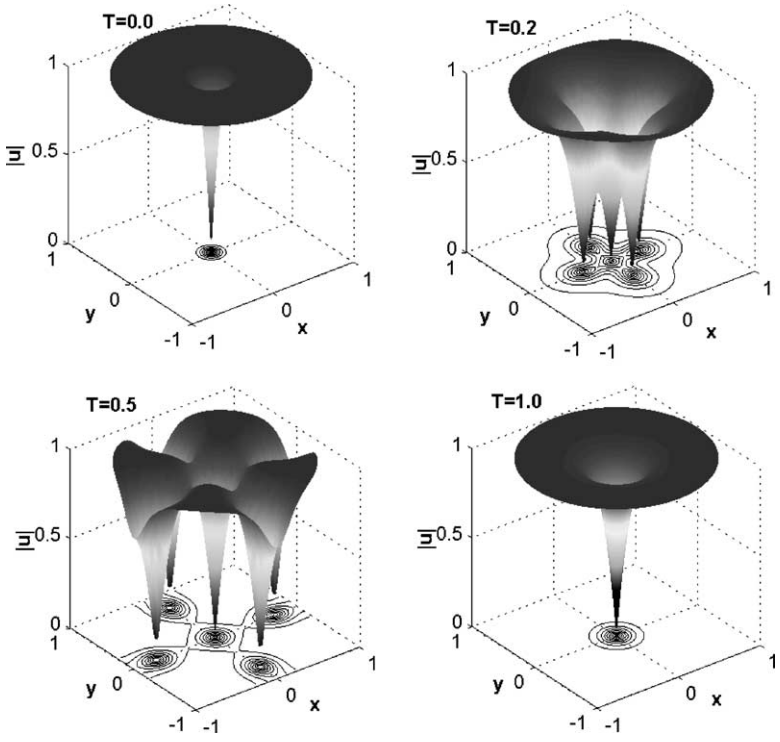

Fig. 3. The contour plots of $|u|$ at different times for the variable diffusion $a(r,\theta) = (r^2 \cos\theta \sin\theta + 1)\,e^r$.

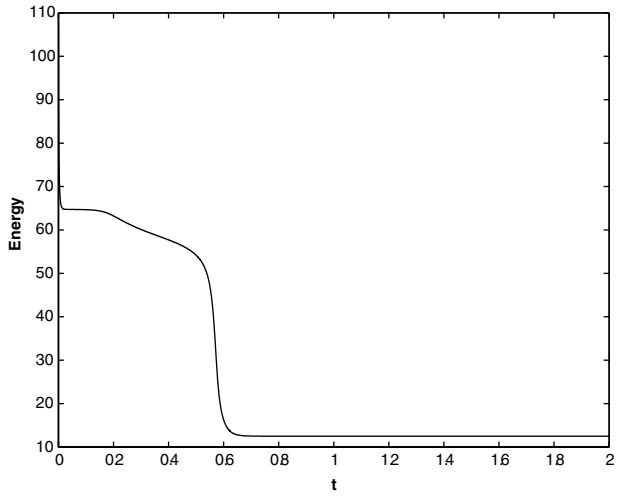

Fig. 4. The time evolution of Ginzburg–Landau energy for the variable diffusion case.

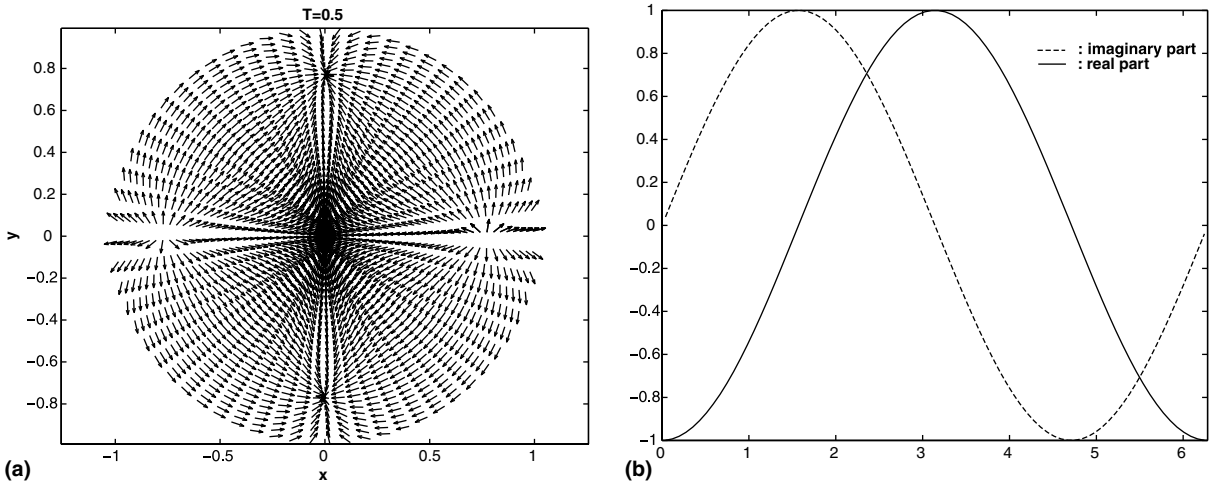

Fig. 5. (a) The vector fields of real and imaginary parts of $u/|u|$ at $T = 0.5$ for the variable diffusion case. (b) The graphs of the real and imaginary parts for $u/|u|$ along the circle near the vortex center at $T = 1$. The real part is denoted by the solid line and the imaginary part is denoted by the dash line.

4. Conclusions

In this paper, we present a fast iterative method for solving the variable coefficient diffusion equation on a unit disk. The equation is written in polar coordinates and is discretized by the standard centered difference approximation under the grid arrangement by shifting half mesh away from the origin so that the coordinate singularity can be easily handled without pole conditions. The resultant matrix is symmetric positive definite so the preconditioned conjugate gradient (PCG) method can be applied. Different preconditioners have been tested for comparison, in particular, a fast direct solver derived by the equation and semi-coarsening multigrid are shown to be scalable preconditioners with the problem size. The present elliptic solver has been applied to study the vortex dynamics of the Ginzburg–Landau equation with a variable diffusion coefficient. Meanwhile, the present numerical scheme can be extended straightforwardly to the similar equation in spherical coordinates and three-dimensional problems.

Acknowledgements

The authors thank the referee for pointing out Ref. [2] and suggesting us to use the multigrid as a preconditioner. The authors also thank Prof. Tai-Chia Lin and Dr. Chin-Tien Wu for useful discussions. The first author was supported by National Science Council of Taiwan under Research Grant NSC-93-2115-M-009-008.

References

[1] O. Buneman, A compact non-iterative Poisson solver, Rep. 294, Stanford University Institute for Plasma Research, Stanford, CA, 1969.

[2] C. Baldwin, P.N. Brown, R. Falgout, F. Graziani, J. Jones, Iterative linear solvers in a 2D radiation-hydrodynamics code: methods and performances, J. Comput. Phys. 154 (1999) 1–40.

[3] J. Adams, P. Swarztrauber, R. Sweet, Fishpack – A package of Fortran subprograms for the solution of separable elliptic partial differential equations, 1980. Available from: <http://www.netlib.org/fishpack>.
[4] F. Bethuel, H. Brezis, F. Hélein, Ginzburg–Landau Vortices, Birkhäuser, Basel, 1994.
[5] X.-Y. Chen, S. Jimbo, Y. Morita, Stabilization of vortices in the Ginzburg–Landau equation with a variable diffusion coefficient, SIAM J. Math. Anal. 29 (1998) 903–912.
[6] H. Chen, Y. Su, B.D. Shizgal, A direct spectral collocation Poisson solver in polar and cylindrical coordinates, J. Comput. Phys. 160 (2000) 453–469.
[7] H. Eisen, W. Heinrichs, K. Witsch, Spectral collocation methods and polar coordinate singularities, J. Comput. Phys. 96 (1991) 241–257.
[8] W. Heinrichs, Spectral collocation schemes on the unit disc, J. Comput. Phys. 199 (2004) 66–86.
[9] W.-Z. Huang, D.M. Sloan, Pole condition for singular problems: the pseudospectral approximation, J. Comput. Phys. 107 (1993) 254–261.
[10] A. Iserles, A First Course in the Numerical Analysis of Differential Equations, Cambridge University Press, Cambridge, 1996.
[11] S. Jimbo, Y. Morita, Stability of non-constant steady state solutions to a Ginzburg–Landau equation in higher space dimensions, Nonlinear Anal. 22 (1994) 753–770.
[12] M.-C. Lai, A note on finite difference discretizations for Poisson equation on a disk, Numer. Methods Partial Differential Eq. 17 (2001) 199–203.
[13] M.-C. Lai, A simple compact fourth-order Poisson solver on polar geometry, J. Comput. Phys. 182 (2002) 337–345.
[14] K. Mohseni, T. Colonius, Numerical treatment of polar coordinate singularities, J. Comput. Phys. 157 (2000) 787–795.
[15] J.C. Neu, Vortices in complex scalar fields, Physica D 43 (1990) 385–406.
[16] S. Schaffer, A semicoarsening multigrid method for elliptic partial differential equations with highly discontinuous and anisotropic coefficients, SIAM J. Sci. Comput. 20 (1998) 228–242.
[17] J. Shen, Efficient spectral-Galerkin methods III: polar and cylindrical geometries, SIAM J. Sci. Comput. 18 (1997) 1583–1604.
[18] J.C. Strikwerda, Finite Difference Schemes and Partial Differential Equations, Wadsworth & Brooks/Cole, 1989, pp. 68.